



HAL
open science

Modelling of a coke oven heating wall

M. Landreau, D. Isler, Alain Gasser, Eric Blond, J.-L. Daniel

► **To cite this version:**

M. Landreau, D. Isler, Alain Gasser, Eric Blond, J.-L. Daniel. Modelling of a coke oven heating wall. 6th European Coke and Ironmaking Congress 2011, Jun 2011, Dusseldorf, Germany. pp.20-25. hal-00634664

HAL Id: hal-00634664

<https://hal.science/hal-00634664>

Submitted on 21 Oct 2011

HAL is a multi-disciplinary open access archive for the deposit and dissemination of scientific research documents, whether they are published or not. The documents may come from teaching and research institutions in France or abroad, or from public or private research centers.

L'archive ouverte pluridisciplinaire **HAL**, est destinée au dépôt et à la diffusion de documents scientifiques de niveau recherche, publiés ou non, émanant des établissements d'enseignement et de recherche français ou étrangers, des laboratoires publics ou privés.

Modelling of a coke oven heating wall

M. Landreau, D. Isler, Centre de Pyrolyse de Marienau (CPM)
A. Gasser, E. Blond, J.-L. Daniel, PRISME Lab.-University of Orléans

ABSTRACT

This work deals with thermomechanical modelling of a coke oven heating wall. The objective is to define the safe limits of coke oven battery operating conditions compatible with a long service life in terms of thermal and mechanical stresses. For this purpose a 3D thermomechanical model of a heating wall taking into account the assembly of bricks and joints was developed with PRISME Laboratory. To build an efficient and complete model, different parameters must be taken into account:

- complexity of the structure: heating walls include flues and are made of masonries with various types of bricks (with various shapes and materials). The presence of joints has a great influence on the wall behaviour since they can open in tension and close in compression;
- brick and joint material behaviours: refractory materials have specific thermo-mechanical behaviours, temperature depending;
- knowledge of thermo-mechanical loading: temperature field, weights of walls, roof and larry car, pre-stresses (anchoring system), lateral pressure due to coal pushing

A 3D heating wall model was developed and allows to take all these parameters into account. The model was created in order to estimate the maximal lateral pressure and to understand mechanism of joints opening. Moreover, the model is based on Fos sur Mer coking plant geometry, and particularly on the battery 3 which was instrumented. Indeed several force sensors have been placed on tie rods, load transmitters and thermocouples on different positions in the brickwork.

Key words : Cokemaking, coke oven, thermomechanical modelling, masonry, homogenization, mechanical tests, finite element method.

1 Introduction

Several studies summed up in [1, 2], were already performed on heating walls. Analytical models have been developed, like the most known Ahlers' model [1]. It allows to obtain the maximal lateral pressure that the heating wall can support (about 10 kPa).

All these analytical works are very simplified since the heating wall was modelled with a beam. An improvement of the previous models was brought by numerical methods, like finite element models [2]. Nevertheless existing models present all some simplifications: joints are not taken into account; the heating wall is represented by an orthotropic shell or in 2D. Thus complete models, which take into account all phenomena, do not exist for the moment.

For this purpose a 3D thermomechanical model of an heating wall taking into account the assembly of bricks and joints was developed. To build this model, different parameters must be taken into account:

- complexity of the structure (figure 1): heating walls include flues and are made of masonries with various types of bricks (with various shapes and materials). Moreover, the presence of joints has a strong influence on wall behaviour since they can open in tension and close in compression;
- bricks and joint material behaviours;
- knowledge of thermomechanical loading: temperature field, weights of walls, roof and larry car, pre-stresses (anchoring system), lateral pressure due to coal pushing.

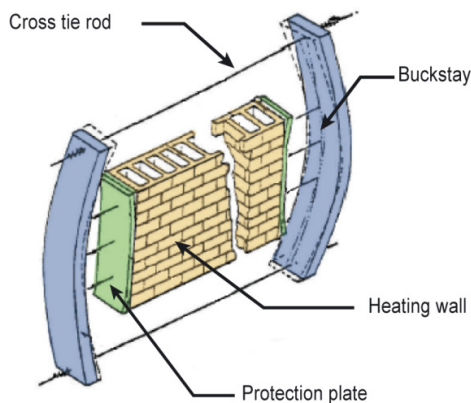


Figure 1 : Heating wall parts.

The model proposed here is an extension of [3] and [4] works on the modelling of mortarless walls to structures with mortar. Their approach is based on periodic homogenization with determination of several equivalent materials according to the opening and closure of joints.

2 Masonry modelling

In order to build a 3D thermomechanical model taking all these parameters into account, a method dealing with periodic homogenization was used. The homogenization method allows identifying the behaviour at the macroscopic scale according to microscopic scale. This determination postulates the existence of a representative elementary volume loaded with homogeneous boundaries conditions [5]. Since masonry arrangement of heating wall is periodical, a periodical homogenization was performed. In order to keep the 3D properties of heating wall, two elementary cells were chosen: the first one for the chamber wall and the second one for the binder as shown in figure 2.

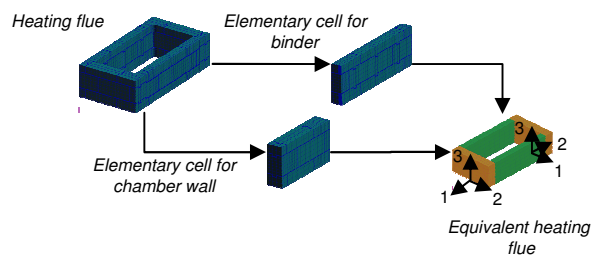


Figure 2 : Elementary cells of heating wall.

During operating conditions, thermal and mechanical loads applied on the heating wall could generate tension regions where joints would be able to open and thus, the masonry behaviour would be different. That is why it is very important to take into account the behaviour of the brick-joint interface. In this study and as presented in numerous approaches, it can be assumed that fractures can develop only in the brick/mortar interface due to the small thickness of mortar [6].

According to opening or closure of bed and head joints, it can be defined 4 different states for each elementary cell. Let us define the state i the state where joints are opened in direction perpendicular to i :

- State 0: joints are closed in all directions;
- State 2: head joints are open and bed joints are closed;
- State 3: bed joints are closed and head joints are open;
- State 2-3: joints are open in all directions.

The figure 3 illustrates the different joint states.

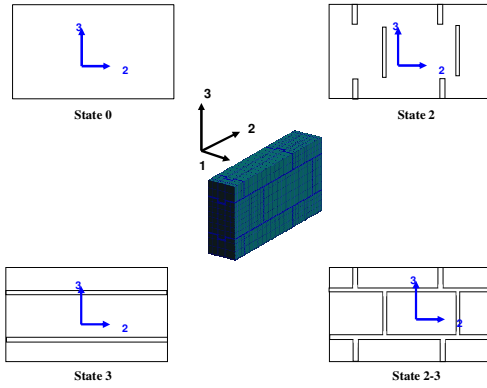


Figure 3 : The different joint states.

Each state corresponds to a different structure and so, an equivalent behaviour must be determined for each pattern [4]. The equivalent material is an orthotropic and elastic material because the distribution of joints is different in the three directions. In order to determine equivalent materials, an inverse method was applied on each elementary cell. Several simulations are necessary to identify them. For each of them the strain energy is calculated through commercial finite element software (ABAQUS) and was compared to the strain energy of the equivalent structure submitted to the same boundary conditions. Thus, the parameters were identified by an inverse method with error minimisation according to Levenberg-Marquardt's algorithm [7]. Once different patterns were defined, a transition criterion was established to go from one state to another. The used criterion is the combination of a tension cut-off criterion and a modified Mohr-Coulomb model for shear:

$$\begin{cases} \sigma_{ii} > f_{tension} \\ \sqrt{\sigma_{ji}^2 + \sigma_{ki}^2} > f_{shear} \end{cases} \quad (1)$$

Where f_{shear} and $f_{tension}$ are the tensile and shear strength of brick-mortar interface. A modification in Mohr-Coulomb criterion allows taking into account hardening of shear limit strength in compression.

$$f_{shear} = c - \frac{1}{2} \tan \Phi (1 - \text{sign}(\sigma_{ii})) \sigma_{ii} \quad (2)$$

$$\text{sign}(\sigma_{ii}) = \begin{cases} 1 & \text{if } \sigma_{ii} > 0 \\ -1 & \text{if } \sigma_{ii} < 0 \end{cases}$$

where c the unit-interface cohesion, and ϕ the friction angle. This model was validated from different mechanical experiments [8].

3 Thermomechanical behaviour of silica brick and mortar

3.1 Thermal and mechanical properties

A good knowledge of materials used for coke oven design is essential to obtain an accurate model. So, mechanical and thermal tests were carried on both silica brick and mortar samples. The Table 1 presents the different tests performed and associated identified properties.

Tests performed	Identified properties
Compression test at 3 temperatures (800, 1080 and 1350 °C)	Young's moduli
Thermal expansion (EN 821-1)	Coefficient of thermal expansion
Differential Scanning Calorimetry	Specific heat
Density (EN 1402-6)	Density
Thermal conductivity (EN 993-15)	Thermal conductivity

Table 1 : List of thermomechanical tests

In this paper, figures 4 and 5 present results of compression and thermal expansion tests. Temperature influence on mechanical behaviour is shown in the figure 4: the more temperature increases, the more material stiffness decreases. Thus, results show a decreasing of elasticity moduli according to temperature, and a ratio of 10 between bricks and mortar Young's modulus.

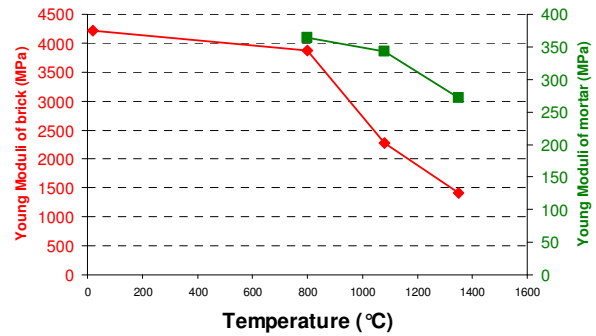


Figure 4 : Comparison of elasticity moduli between brick and mortar.

Thermal expansion curves for the two materials were recorded during heating and cooling (Figure 5). Brick and mortar behaviour is the same on the whole: a high expansion up to 500°C, then stabilization around 1.1%. These two curves are closed which involves slight thermomechanical stresses in brick-mortar interface.

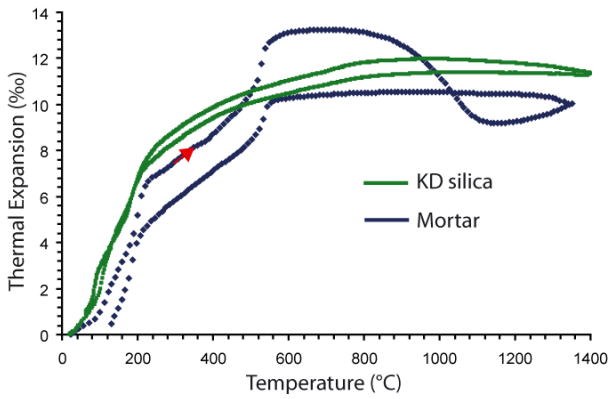


Figure 5 : Thermal expansion for brick and mortar.

3.2 Characterisation of brick/mortar interface

Transition criterion developed in these works is dependant of several parameters like tensile strength f_t , cohesion c and friction angle ϕ . These different parameters have to be determined that is why two different tests were developed.

The first one is a compression/shear test which allows to identify Mohr-Coulomb parameters. Different tests were performed at different temperatures and for different angles α of mortar joint, as shown on Figure 6. Thus all samples are heated until 1000°C during 1 hour, then tests were performed at 3 different temperatures (800, 1080 and 1350 °C).



Figure 6 : Compression/shear tests for different angles (45, 55 and 65°). Specimens after failure.

Results of these different tests are summarized in the Table 3. It can be noticed that there is a decrease of cohesion c according to temperature, but a weak influence of this temperature on friction angle ϕ . Moreover, as illustrated on figure 6, we can notice that fractures develop in the brick/mortar interface due to the weak cohesion between these materials.

	800°C	1080°C	1350°C
c (MPa)	0.48	0.244	0.217
$\tan \phi$	0.903	0.825	0.85

Table 2: Identification of Mohr-Coulomb parameters according to temperature.

A second test was developed in order to identify tensile strength f_t . Characterisation of this parameter for masonry material is very complex. In fact, different problems have to be solved: clamping specimen,

applying a uniaxial load and performing tests at high temperatures [8]. That is why a new test was developed, and for the moment a value of 0.2 MPa was obtained only at room temperature.

4 Homogeneous equivalent materials for the heating wall

4.1 Mechanical properties

As presented before, masonry mechanical behaviour is function of joints opening and temperature. Equivalent behaviours were determined for each case for 3 temperatures (800, 1080 and 1350°C). On the Table 3, only elasticity moduli are displayed. The equivalent parameters are coherent: the Young's moduli are inferior to brick modulus because of presence of joints. Moreover in state 2, Young's modulus in direction of opening is the lower (it is due to the lack of mortar in this direction) and in state 3, elasticity modulus in direction three is equal to zero because there is no stiffness in this direction.

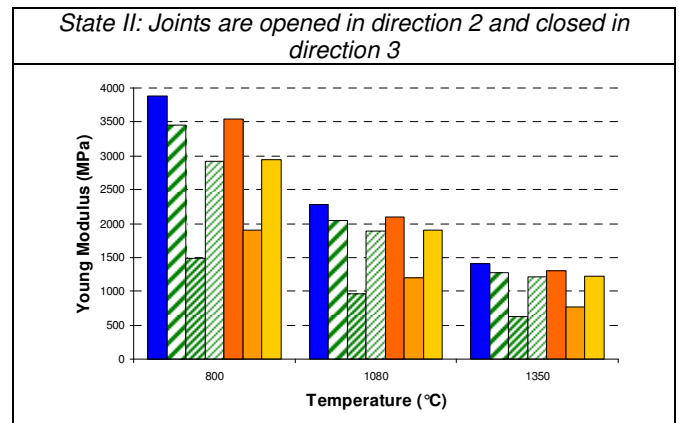
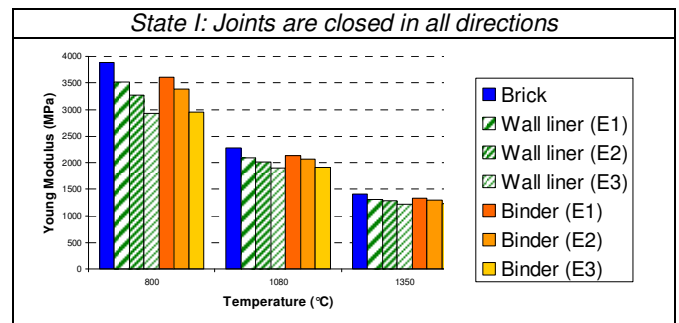


Table 3: Set of equivalent parameters for different joint states.

4.2 Thermal properties

To model thermomechanical behaviour of heating wall, equivalent thermal parameters have to be determined for different states too. Due to experimental uncertainties values for different thermal properties of

brick and mortar are similar, ., The different thermal parameters were identified by different methods:

- the effective thermal conductivity was calculated by a self consistent method [9] ,
- the density and specific heat were calculated by an average per unit volume,
- the expansion coefficients were identified by the same method than mechanical parameters, i.e. by inverse identification.

For example, Figure 7 presents results of effective thermal conductivity according to temperature.

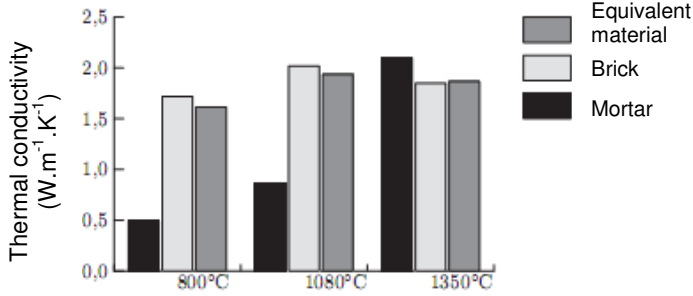


Figure 7: Equivalent thermal conductivity.

5 Simulation of the heating wall

All tools which allow to model thermomechanical behaviour were defined previously. This last part is so devoted to model the heating wall. In a first time, geometry and mesh are presented, secondly boundary conditions and loads are explained and finally, results of modelling are showed.

5.1 Geometry and mesh

The established model is based on geometry of heating wall 305 of Fos sur Mer coking plant. This model takes into account different parts: the sole is represented by an analytical rigid solid; the roof is not drawn but its effect is modelled thanks to boundary conditions. With regards to metallic parts, only protection plates are modelled with an isotropic elastic behaviour. The heating wall is represented with the two equivalent homogeneous materials (for the chamber and binder wall) which have an orthotropic behaviour. Behaviour of insulating bricks is taken into account just as heating wall taper. Figure 8 illustrates the heating wall modelling.

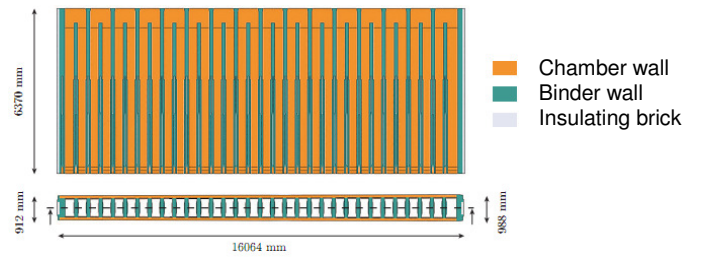


Figure 8 : Heating wall model.

Mesh of this structure was realised with 8 nodes elements and so, global mesh is made of 501,000 elements.

5.2 Boundary conditions and loads

The calculation of this large structure was realised in two steps: thermal then mechanical simulations. Afterwards, a description of these different loads is presented.

5.2.1 Thermal

Thermal load can be divided into four types: temperature in the heating flues (measured), exchange between coke and heating wall (estimated), exchange between protection plate and surrounding air (estimated) and finally exchange between heating wall and protection plate (estimated).

Heating flues

Thanks to Pyrofil measures, different temperature profiles can be applied inside the different heating flues. The reversals every 20 min are taken into account thanks to a routine in ABAQUS.

Exchange between protection plate and surrounding air

In order to respect thermal exchanges, a coefficient of global exchange k_{global} was inputted. This coefficient is defined such way that if ϕ is the flux density which goes through protection plate to air, the following relation can be written:

$$\phi = k_{global} (T_{protection\ plate} - T_{air}) \quad (3)$$

This coefficient is obtained by adding thermal resistance of air and buckstay. Writing down h_{air} the thermal exchange coefficient of air, $e_{buckstay}$ the thickness of buckstay and $\lambda_{buckstay}$ its conductivity, global exchange coefficient is given by:

$$\frac{1}{k_{global}} = \frac{1}{h_{air}} + \frac{e_{buckstay}}{\lambda_{buckstay}} \quad (4)$$

Numerical values are summarized in Table 4.

h_{air}	$e_{buckstay}$	$\lambda_{buckstay}$	T_{air}	k_{global}
20 W.m ⁻² .K ⁻¹	685 mm	60 W.m ⁻¹ .K ⁻¹	25°C	16.3 W.m ⁻² .K ⁻¹

Table 4 : Properties for thermal exchange between protection plate and surrounding air.

Exchange between heating wall and protection plate

During battery construction, a ceramic layer is placed between protection plates and heating wall, just as chamotte bricks. Since these elements are not drawn in this model, their thermal properties are taken into account thanks to thermal contact conditions. The thermal behaviour of ceramic layer and chamotte bricks is represented by thermal conductivity evolution versus thickness. The properties of this exchange are summarized in Table 5.

e (mm)	λ (e) (W.m ⁻¹ .K ⁻¹)
0	∞
1	0.5
30	0.5
31	1.2
100	1.2
∞	0

Table 5 : Thermal exchange between heating wall and protection plates.

Exchange between coke and heating wall

Thermal exchange between coke and heating wall was still modelled with equation (3). Nevertheless in this load, the global coefficient is supposed constant (and equal to 100 W.m⁻².K⁻¹) and it is the temperature of coke which progresses. 2D model of coal heating were build in order to identify this evolution according to height and time. The results are displayed on figure 9.

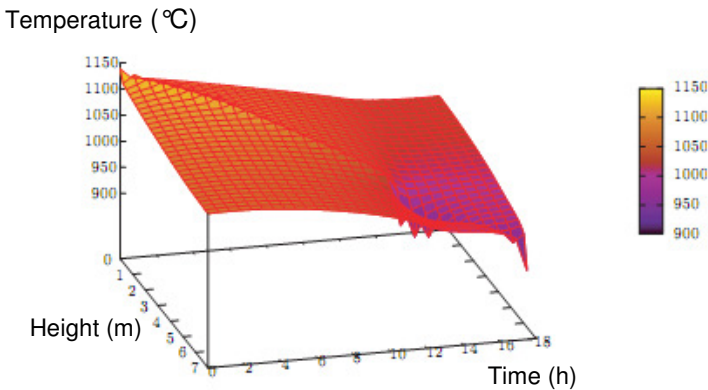


Figure 9 : Evolution of temperature according time and height.

Thus, the combination of these different boundary conditions allows calculating the temperature field in the heating wall during coking time.

5.2.2 Mechanical

In the second step, this temperature field is used in a thermomechanical model to locate the possible joint openings. In this mechanical step, all loads (weight of roof, anchoring system, lateral pressure) are applied on the structure. Thus, a vertical pressure of 0.1 MPa is applied on the heating wall to represent the weight of roof. The efforts due to anchoring system are applied on the protection plate and are equal to constructor values. Dealing with lateral pressure, the distribution of swelling pressure along the height of the wall was introduced as nearly triangular shaped, with a value of 6 kPa at 6.4m and a maximum pressure at the bottom of the charge (15 kPa). Moreover, a shift is applied to account charging sequence as illustrated on figure 10.

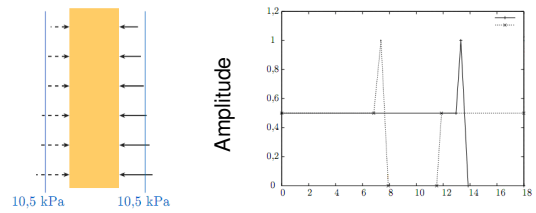


Figure 10 : Coke swelling pressure.

5.3 Results

The figure 11 presents results of thermal calculations on the heating wall. This picture shows the different reversal in heating flues. This heating by twin flue wall allows to obtain a homogeneous temperature field in the masonry. The coldest temperatures (around 300°C) are located in heads of heating wall due to air whereas the hottest are placed at the bottom of flues near the flame (around 1300°C).

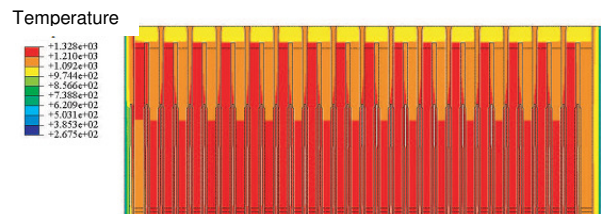


Figure 11 : Temperature field in the heating wall.

For the mechanical part, three different models were studied with the same set of boundary conditions and loads. In the first one, thermomechanical behaviour of brick is applied to the structure (model MB); in the second one, equivalent parameters identified for chamber and binder walls (for closed joints) are applied (model MH) and finally, in the last case, equivalent parameters are also applied plus the opening criterion in order to account joint openings (model MHC).

During calculations, stress profiles are recorded according a horizontal path at middle height of wall. As presented on figure 12, normal stress profiles are plotted at once after the coal charging and peak of swelling pressure.

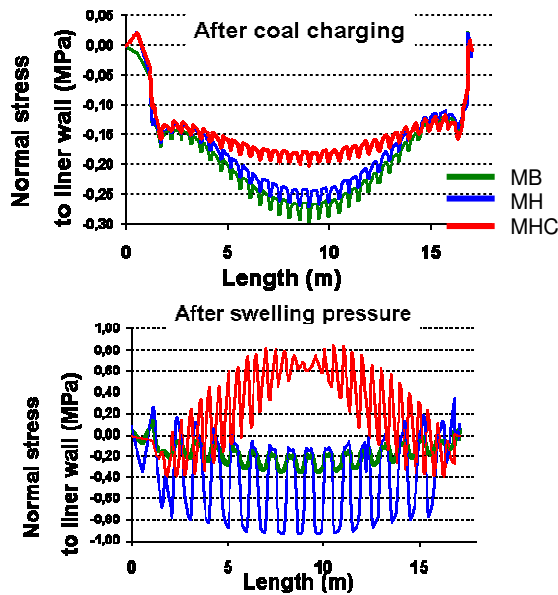


Figure 12 : Comparison of stress profiles according to coking time.

After the coal charging, it can be noticed that there is a bending of heating wall due to thermal gradient in the structure. In fact, a chamber wall is colder than the other one due to the charging sequence. Normal stress evolution for the 3 models is similar, just as the distribution. The simplest models (MB and MH) overestimate stresses in masonry since they don't take into account joint openings. Thus, the model MB overestimates stresses of 10% with respect of MH model and 40% with respect of MHC model.

After several hours, peak of coke swelling pressure appears and implies joint openings as illustrated on figure 11 (MHC model). These vertical joint openings start in the middle of the structure and spread to heating wall heads. They are located at the level of binder walls and are in agreement with damages observed in coking plants. These openings which cannot be reproduced by MB and MH models, cause stress redistribution as plotted on figure 12. Thus, the obtained stress profile with MHC model is completely different than for the simplest models.

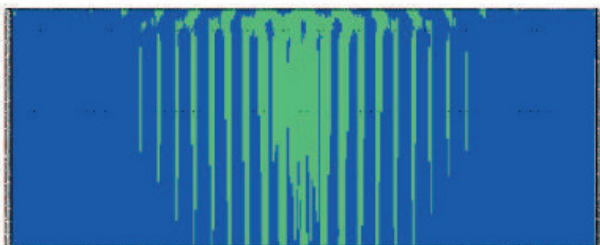


Figure 13 : Vertical joint openings in the heating wall.

Another calculation was performed without applying swelling pressure (only thermal stresses), and no joint

openings were obtained. Thus maximal lateral pressure is included in the following interval [0; 10.5 kPa]. Further calculations are scheduled in order to obtain the danger point of damaging.

Conclusion

This approach allows to model a 3D heating wall taking all thermomechanical loads into account. The model presented here was developed in order to estimate the maximal lateral pressure and to understand mechanism of joints openings too. Moreover several force sensors were placed on tie rods and load transmitters at different height and they will be used to validate the model.

Acknowledgements

The authors would like to thank ArcelorMittal and European Union for their technical and financial supports for COOL research project of RFCS program.

References

- [1] Dürselen H., 1999. Some critical considerations concerning new theoretical models for the stability of coke oven heating walls, *Cokemaking International*, 1, 40-48.
- [2] McDermott J. F., 1990. Capacity of 6-metre coke-oven walls to resist unbalanced lateral pressure, *Iron and Steel Society*.
- [3] Gasser A., Terny-Rebeyrotte K., Boisse P., 2004. Modelling of joint effects on refractory lining behaviour. *J. Mater.: Design Appl. (IMechE)* 218, 19-28.
- [4] Nguyen T., Blond E., Gasser A., Prietl T., 2009. Mechanical homogenisation of masonry wall without mortar. *European Journal of Mechanics - A/Solids* 28 (3), 535-544.
- [5] Bornert M., Bretheau T., Gilormini P., 2006. *Homogenization in Mechanics of Materials*. Iste Publishing Company.
- [6] Luciano R., Sacco E., 1997. Homogenization technique and damage model for old masonry material. *International Journal of Solids and Structures* 34 (24), 3191-3208.
- [7] Marquardt D., 1963. An algorithm for least squares estimation of non linear parameters. *J. Appl. Math* 11, 431-441.
- [8] Landreau M., 2009. *Thermomechanical modelling of a coke oven heating wall*. PhD thesis, Insitut Prisme – Université d'Orléans (in French)
- [9] Carson, J.K., Lovatt, S.J., Tanner, D.J., Cleland, A.C., 2005 Thermal conductivity bounds for isotropic, porous materials. *International Journal of Heat and Mass Transfer*, 48(11):2250-2158,